Molecular Mechanics Studies of Model Iron(III) Transferrin Complexes *in Vacuo* and in Aqueous Solution

Wangkan Lin, William J. Welsh,* and Wesley R. Harris

Department of Chemistry, University of Missouri—St. Louis, St. Louis, Missouri 63121

Received June 9, 1993®

A molecular mechanics (MM) investigation of low-molecular-weight ferric chelates has been conducted to develop iron parameters appropriate to the AMBER all-atom force field for subsequent MM studies of ferric transferrin. These force-field parameters were derived (1) by fitting of the crystal structure geometries of the Fe(III) complexes of ethylenebis(*o*-hydroxyphenylglycine) (EHPG), 1,4,7-triazacyclononane-1,4,7-triacetic acid (TCTA), and 1,5-diazapentane-1,1,5,5-tetraacetic acid (TRDTA), (2) by conducting a statistical analysis of 44 crystal-structure geometries of Fe(III) complexes extracted from the Cambridge Structural Database, and (3) by making comparisons with published force-field parameters relevant to transition metal complexes. Energy minimized molecular structures and conformational energies of the (*R,R*), (*R,S*), and (*S,S*) isomers of EHPG were calculated both *in vacuo* and in aqueous solution estimated (1) crudely using a distance-dependent dielectric constant ϵ and (2) more rigorously using the generalized Born/surface area (GB/SA) continuum treatment of Still. Rms deviations between the present GB/SA-calculated and published crystal-structure geometries for the *R,R rac* isomer of Fe^{III}EHPG are 0.044 Å for bond lengths, 3.15° for bond angles, and 6.9° for torsion angles. The corresponding rms deviations for the *R,S meso* isomer are 0.025 Å for bond lengths, 2.78° for bond angles, and 5.5° for torsion angles. Similar rms deviations were obtained for the Fe^{III}TCTA, Fe^{III}TRDTA, and Fe^{III}EDDDA [(ethylenediamine-*N,N'*-diaceto-*N,N'*-di-3-propionato)iron(III)] complexes. The calculated conformational energies for the Fe^{III}EHPG complexes show that (1) the order of increasing stability is *S,S rac* < *R,S meso* < *R,R rac*, (2) this order does not change whether calculated *in vacuo* or in aqueous solution, and (3) aqueous solvation reduces the energy differences among the three conformers. The GB/SA-calculated energy difference of 2.89 kcal/mol between the *R,R rac* and *R,S meso* conformers compares well with experimentally measured stability constants corresponding to $\Delta(\Delta G)$ of 1.65 and 3.10 kcal/mol. The failure to observe the *S,S rac* conformer in the crystal is attributed to its inherent instability rather than to unfavorable crystal packing. The calculated order of stability for the three Fe^{III}EDDDA conformers was *trans*-(O_6) < *trans*-(O_5,O_6) < *trans*-(O_5), of which the *trans*-(O_5) conformer is the only form observed in the crystal. The present MM calculations predict that optimum stability is achieved when the ligands adopt an equitorial coordination plane containing a 6, 5, 6 combination of chelate-ring sizes, with two 5-membered axial chelate rings.

Introduction

Serum transferrin (Tf) is the iron transport protein in a wide variety of species.[1,2] The protein binds ferric ion strongly enough to prevent hydrolysis at physiological pH and to deny essential iron to invading bacteria. The protein also provides a mechanism for regulating cellular iron uptake by binding to specific outer membrane receptors for transport into the cell.

Because it exists free in serum, transferrin is a potential target for drugs to treat iron overload in patients on long-term transfusion therapy. However, iron removal by a wide variety of chelating agents is quite slow at physiological pH.[3-10] Kinetic studies on iron removal from this protein have often been interpreted in terms of an as yet uncharacterized rate-determining conformational change.[3-8] Recently determined crystal structures of the diferric and apo forms of the closely related protein lactoferrin[11-13] (Lf) show that the removal of the iron causes a significant conformational change in the N-terminal lobe but not in the C-terminal lobe. This finding is viewed as supportive of a mechanism in which iron release is mediated by a conformational change. However, iron release is likely to be gated by a more limited transition of ferric Tf to a partially open form. Such a partially open form of ferric Tf has yet to be characterized spectroscopically or crystallographically. Thus a more complete analysis of the solution conformations of diferric transferrin is needed.

Molecular mechanics (MM) has become a powerful computational tool for investigating conformations of metal complexes.[14-16] The technique relies on the availability of a suitable force field, which is used to calculate the conformational energies by summing intramolecular effects such as bond stretching, bond-angle bending, and torsional rotation, as well as van der Waals and electrostatic interactions. For extensions to solution studies, it is now possible to quantify intermolecular solvent effects beyond the mere assignment of a bulk dielectric constant ϵ. Numerous computational methodologies are available today for treating the solvent molecules, either in an explicit manner or as a continuum.

* Author to whom correspondence should be addressed.

® Abstract published in *Advance ACS Abstracts,* February 1, 1994.

(1) Harris, D. C.; Aisen, P. In *Iron Carriers and Iron Proteins*; Loehr, T. M., Ed., VCH Publishers: New York, 1989; pp 239-352.
(2) Brock, J. H. In *Metalloproteins, Part II*; Harrison, P., Ed., Macmillan: London, 1985; pp 183-262.
(3) Cowart, R. E.; Swope, S.; Loh, T. T.; Chasteen, N. D.; Bates, G. W. *J. Biol. Chem.* **1986**, *261*, 4607.
(4) Cowart, R. E.; Kojima, N.; Bates, G. W. *J. Biol. Chem.* **1982**, *257*, 7560.
(5) Kretchmar, S. A.; Raymond, K. N. *J. Am. Chem. Soc.* **1986**, *108*, 6212.
(6) Bali, P. K.; Harris, W. R.; Nesset-Tollefson, D. *Inorg. Chem.* **1991**, *30*, 502.
(7) Marques, H. M.; Watson, D. L.; Egan, T. J. *Inorg. Chem.* **1991**, *30*, 3758.
(8) Bertini, I.; Hirose, J.; Luchinat, C.; Messori, L.; Piccioli, M.; Scozzafava, A. *Inorg. Chem.* **1988**, *27*, 2405.
(9) Baldwin, D. A. *Biochim. Biophys. Acta* **1980**, *623*, 183.
(10) Konopka, K.; Bindereif, A.; Nielands, J. B. *Biochemistry* **1982**, *21*, 6503.
(11) Anderson, B. F.; Baker, H. M.; Dodson, E. J.; Norris, G. E.; Rumball, S. V.; Waters, J. M.; Baker, E. M. *Proc. Natl. Acad. Sci. U.S.A.* **1987**, *84*, 1769.
(12) Anderson, B. F.; Baker, H. M.; Norris, B. E.; Rumball, S. V.; Baker, E. N. *Nature* **1990**, *344*, 784.
(13) Anderson, B. F.; Baker, H. M.; Norris, B. E.; Rice, D. W.; Baker, E. N. *J. Mol. Biol.* **1989**, *209*, 711.
(14) Hancock, R. D. *Acc. Chem. Res.* **1990**, *23*, 253.
(15) Brubaker, G. R. *Coord. Chem. Rev.* **1984**, *53*, 1.
(16) Hancock, R. D. *Prog. Inorg. Chem.* **1989**, *37*, 187.

0020-1669/94/1333-0884$04.50/0

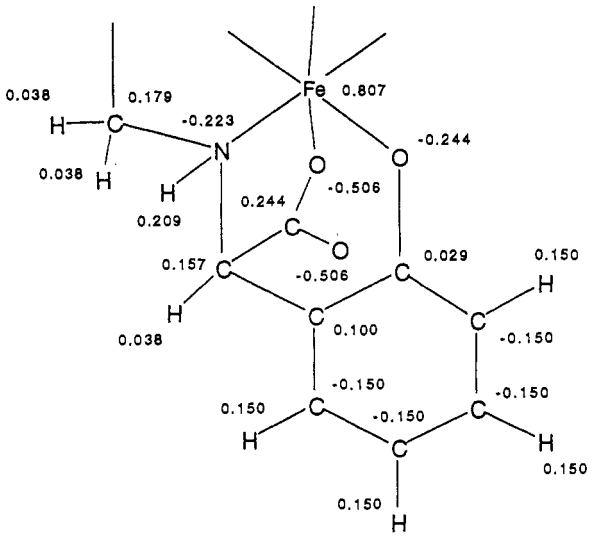

Figure 1. Assignment of atomic partial charges in the Fe^{III}EHPG complexes.

The major obstacle to applying computational chemistry methods for the study of transferrin solution conformations is the lack of well-tested force field parameters for the high-spin, non-heme, ferric ions bound to this protein. Therefore, we have initiated a molecular modeling investigation of low-molecular-weight ferric chelates to develop suitable iron parameters for subsequent MM studies of ferric Tf.

Transferrin contains two high-affinity iron binding sites. Each ferric ion is directly coordinated to the phenolate side chains of two tyrosine residues, the imidazole side chain of a histidine, and the carboxylate group of an aspartic acid.[17-18] The remaining two coordination sites are occupied by a bidentate carbonate anion, which is also hydrogen bonded to polar and charged groups of the protein.[13,18]

The phenolic ligand ethylenebis(*o*-hydroxyphenylglycine) (EHPG) has often been used as a model for the transferrin binding site. EHPG provides an excellent model for methods that are most sensitive to the iron–phenolate interactions. There is an excellent match between the difference UV spectra of the transferrin and EHPG complexes among a wide variety of metal ions.[19] The charge-transfer spectra of Fe(III)–EHPG and Mn(III)–EHPG complexes are very similar to the corresponding Tf and Lf complexes,[20-22] and there are strong similarities in the resonance Raman spectra of Fe(III)–EHPG and Fe(III)–Tf complexes.[23a] The Fe(III)–EHPG and Fe(III)–Tf complexes also have similar EPR *g* values[21,22] as well as similar isomer shifts and quadrapole splittings in the Mossbauer spectra.[22,23b] Thus EHPG is an excellent model system for developing the appropriate force field parameters for high-spin ferric ion coordinated to phenolic groups.

EHPG has two asymmetric carbons; thus the iron complex can adopt three different configurations designated (*R*,*R*), (*R*,*S*), and (*S*,*S*) as shown in Figure 2. The crystal structures[25] and stability constants[26] for the (*R*,*R*) and (*R*,*S*) conformers are available. In contrast, the corresponding (*S*,*S*) conformer has never been reported.

In the present study, Fe(III)-related molecular mechanics parameters have been developed for use in the AMBER all-atom force field.[24] This enhancement of the AMBER force field enabled us to evaluate the relative stabilities of the three possible conformers of ferric EHPG. These computational results are compared with the experimentally-measured stability constants for the (*R*,*R*) and (*R*,*S*) complexes. The structurally analogous iron complexes of 1,4,7-triazacyclononane-1,4,7-triacetic acid (TCTA), 1,5-diazapentane-1,1,5,5-tetraacetic acid (TRDTA), and ethylenediamine-*N*,*N*′-diaceto-*N*,*N*′-di-3-propionic acid (EDDDA) were also selected for inclusion in the development of the force-field parameters.

Results

Development of Force-Field Parameters. The set of Fe(III)-related paameters which we added to the all-atom AMBER force field[24] are listed in Table 1. The derivation of these parameters was based on three sources: (1) fitting of the crystal structure geometries of the Fe^{III}EHPG complexes (including three structures and two conformations), the Fe^{III}TCTA complex, and the Fe^{III}TRDTA complex; (2) a statistical analysis of 44 crystal structure geometries of Fe(III) complexes; and (3) published force-field parameters related to transition metal complexes. These published parameters apply to the AMBER force field[24] as well as to other force fields.[27,28]

The relevant structural data were obtained by searching the Cambridge Structural Database (CSD).[29] For the present purpose, our search was confined to those complexes which contain (1) a six-coordinate Fe(III), (2) exclusively nitrogen or oxygen atoms as coordinating atoms, and (3) at least one carbon atom bonded to the coordinating atom. Among the structures identified by the CSD search are many porphyrin derivatives. We decided to exclude these porphyrin complexes since their ligands have a rigid coordination structure; consequently, they may not adequately represent the geometry of a rather flexible ligand.

The remaining 44 CSD structures were further divided into a high-spin group and a low-spin group. The major structural difference among them is the bonding distances. For example, the Fe(III)–N(sp^3) distance is about 2.23 Å in the high-spin complexes but only 2.03 Å in the low-spin complexes. A statistical analysis carried out on the bond lengths of these structures is summarized in Table 2. This structural information was invaluable in assessing the relationship between structural geometry and the atom types.

Among the 44 CSD structures, we selected in particular the Fe^{III}EHPG, Fe^{III}TCTA, and Fe^{III}TRDTA complexes as our structural "basis set" for parameter development. These complexes do not contain any metal-containing bonds other than Fe(III)–N(sp^3), Fe(III)–O(phenolic), and Fe(III)–O(carboxylate) bonds. Furthermore, they are all high-spin complexes devoid of any ligand field stabilization energy (LFSE). Since an octahedral geometry is not stabilized by LFSE in these cases, we adopted "soft" bending force constants for the X–Fe–X angles (where

(17) Bailey, S.; Evans, R. W.; Garratt, R. C.; Gorinsky, B.; Hasnain, H.; Horsburgh, C.; Jhoti, H.; Lindley, P. F.; Mydin, A.; Sarra, R.; Watson, J. L. *Biochemistry* **1988**, *27*, 5804.
(18) Sarra, R.; Garratt, R.; Gorinsky, B.; Jhoti, H.; Lindley, P. *Acta Crystallogr.* **1990**, *B46*, 763.
(19) Pecoraro, V. L.; Harris, W. R.; Carrano, C. J.; Raymond, K. N. *Biochemistry* **1981**, *20*, 7033.
(20) Patch, M. G.; Simolo, K. P.; Carrano, C. J. *Inorg. Chem.* **1982**, *21*, 2972.
(21) Patch, M. G.; Simolo, K. P.; Carrano, C. J. *Inorg. Chem.* **1983**, *22*, 2630.
(22) Ainscough, E. W.; Brodie, A. M.; Plowman, J. E.; Brown, K. L.; Addison, A. W.; Gainsford, A. R. *Inorg. Chem.* **1980**, *19*, 3655.
(23) (a) Gaber, B. P.; Miskowski, V.; Spiro, T. G. *J. Am. Chem. Soc.* **1974**, *96*, 6868. (b) Spartalian, K.; Carrano, C. J. *J. Chem. Phys.* **1983**, *78*, 4811.
(24) Weiner, S. J.; Kollman, P. A.; Nguyen, D. T.; Case, D. A. *J. Comput. Chem.* **1986**, *7*, 230.
(25) Bailey, N. A.; Cummins, D.; McKenzie, E. D.; Worthington, J. M. *Inorg. Chim. Acta* **1981**, *50*, 111.
(26) Bannochie, C. J.; Martell, A. E. *J. Am. Chem. Soc.* **1989**, *111*, 4735.
(27) (a) Adam, K.; Antolovich, M.; Bigden, L. G.; Lindoy, L. F. *J. Am. Chem. Soc.* **1991**, *113*, 3346. (b) Lin, W.; Alcock, N. W.; Busch, D. H. *J. Am. Chem. Soc.* **1991**, *113*, 7603.
(28) (a) Vedani, A.; Huhta, D. W. *J. Am. Chem. Soc.* **1990**, *112*, 4759. (b) Vedani, A. *J. Comput. Chem.* **1988**, *9*, 269.
(29) (a) Allen, F. H.; Bellard, S.; Brice, M. D.; Cartwright, B. A.; Doubleday, A.; Higgs, H.; Hummelink, T.; Hummelink-Peters, B. G.; Kennard, O.; Motherwell, W. D. S.; Rodgers, J. R.; Watson, D. G. *Acta Crystallogr.* **1979**, *B35*, 2331. (b) Allen, F. H.; Kennard, O.; Taylor, R. *Acc. Chem. Res.* **1983**, *16*, 146.

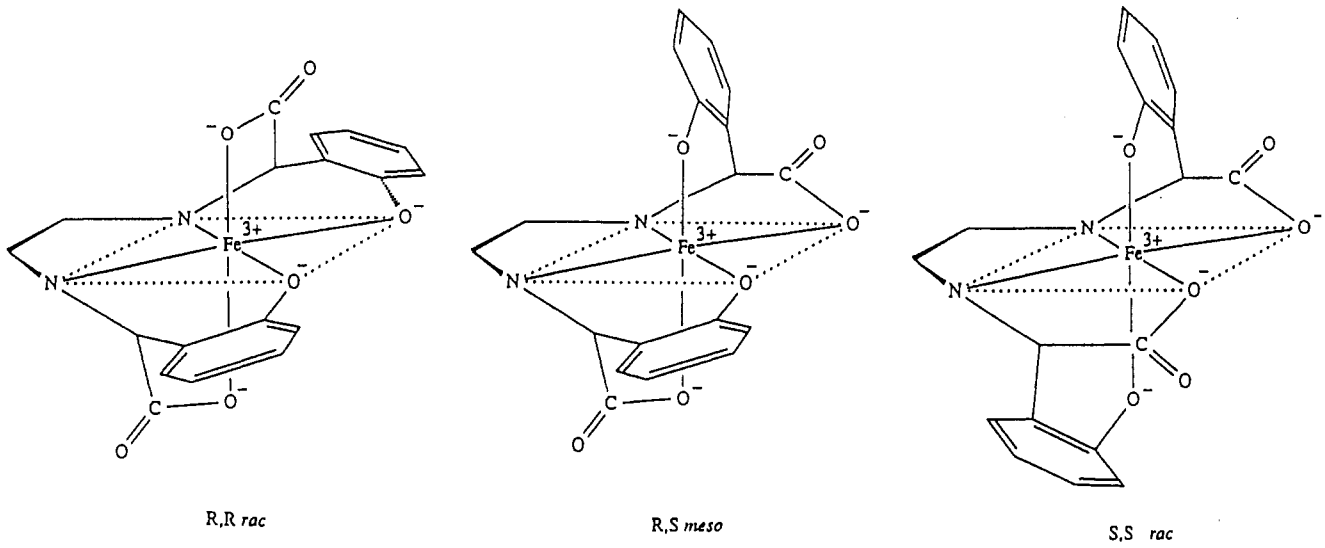

Figure 2. Illustration of the three possible conformers of the Fe^{III}EHPG complex.

Table 1. Selected Force Field Parameters[a]

Bonds

	k (kcal/mol/Å²)	ref value (Å)
Fe(III)–N(sp^3)	110.0	2.240
Fe(III)–O(phenolic)	110.0	1.910
Fe(III)–O(carboxylate)	110.0	2.020

Angles[b]

	k (kcal/(mol/rad²)	ref value (deg)
Fe(III)–O(phenolic)–C(sp^2)	60.0	125.0
Fe(III)–O(carboxyl)–C(sp^2)	70.0	120.0
Fe(III)–N(sp^3)–X	50.0	109.5
N(sp^3)–Fe(III)–O(all types)	15.0	90.0; 180.0
O(phen)–Fe(III)–O(phen)	15.0	90.0; 180.0

Torsions

	k_1	k_2	k_3
X–Fe(III)–X–X	0.00	0.00	0.00

Nonbonded

	σ (Å)	ϵ (kcal/mol)
Fe(III) atom	2.08	0.134

[a] "X" refers to any specified atom. These parameters were obtained (1) by fitting to the subject crystal structures and (2) from the following published sources: Lopez, M.; Kollman, P. *J. Am. Chem. Soc.* **1989**, *111*, 6212. Still, C. *Macromodel* Manual; Columbia University: New York. Weiner, S.; Kollman, P.; Case, D.; Singh, U.; Ghio, C.; Alagona, C.; Profeta, S.; Weiner, P. *J. Am. Chem. Soc.* **1984**, *106*, 765. Weiner, S. J.; Kollman, P. A.; Nguyen, D. T.; Case, D. A. *J. Comput. Chem.* **1986**, *7*, 230. Curtiss, L.; Halley, J.; Hautman, J.; Rahman, A. *J. Chem. Phys.* **1987**, *84*, 2319.

"X" represents any atom type). We also note that the present force field parameters pertain exclusively to the Fe(III)–N(sp^3) bond type and do not in general extend to the Fe(III)–N(sp^2) bond type.

Our approach for deriving the force field parameters is illustrated in the following example. In a recent study of a metalloporphyrin–ligand system, Lopez and Kollman[30] implemented the AMBER force field using Fe–N and Fe–O bond-stretching force constants of 50.0 kcal/(mol Å²). However, we found this magnitude to be too low when applied in the present case. Specifically, our calculated Fe–N distances would vary more than 0.2–0.3 Å in the fitted complexes whereas the observed deviations are normally 0.1 Å or less. Other studies have reported that the Fe–N distances tend to deviate less for Fe(III) complexes than for Fe(II) complexes[31] and that the "breathing" force constants of the Fe–H_2O (solvent shell) in a Fe(III) system are about 2 times larger than those in a corresponding Fe(II) system.[32] In accordance with these differences, we set the Fe(III)–N and Fe(III)–O bond-stretching force constants to a larger value (110.0 kcal/(mol Å²)).

Table 2. Statistical Analysis of Bond Lengths in the Crystal Structures of Fe(III) Complexes

bond	length (Å)	deviation (Å)	sample size[a]
Fe–N(sp^2), high spin	2.120	0.030	14
Fe–N(sp^2), low spin	1.946	0.025	11
Fe–N(sp^3), high spin	2.228	0.058	16
Fe–N(sp^3), low spin	2.029	0.039	9
Fe–O(phenolic)	1.906	0.026	24
Fe–O(carboxylate)	2.001	0.040	15

[a] Number of structures studied. For structures containing more than one molecule in the unit cell, an average bond length was calculated and then taken as one entry in the statistical analysis.

The development of force field parameters is often hampered by the paucity of relevant experimental data. A pertinent example is the van der Waals parameters for Fe(III). Nevertheless, we found that the calculated structures were largely insensitive to small variations in the values chosen for the well depth and hardness parameters ϵ and σ. The chief explanation stems from the absence of any close (i.e., <4 Å) nonbonded contacts with the metal center among our fitting complexes. Accordingly, we set these parameters to the values listed in Table 1.

The point charges assigned to the atoms in the ligand were taken from the AMBER force field.[24] The charges on the coordinated atoms and transition metal were then chosen to best fit the experimental geometry while maintaining the formal ionic charge of the complex. An example of the assignment of the charges is given in Figure 1. It should be noted that the charge assigned to the iron atom is noticeably smaller than its +3 formal charge. Exploratory calculations were carried out to assign a higher charge to the transition metal and, correspondingly, to adjust the charges on coordinated atoms. However, these deliberations failed to show improvements in the fitting to the crystal structures. We note that Lopez and Kollman[30] similarly adopted small values for the partial charge of iron(II) (viz., 0.20 e; 0.27 e) in a combined molecular mechanics–molecular dynamics study of iron(II) porphyrin systems.

The Fe^{III}EHPG Complexes: Structure and Conformation. The molecular structures of the possible conformers of EHPG

(30) Lopez, M.; Kollman, P. *J. Am. Chem. Soc.* **1989**, *111*, 6212.

(31) Sim, P. G.; Sinn, E.; Petty, R. H.; Merrill, C. L.; Wilson, L. J. *Inorg. Chem.* **1981**, *20*, 1213.

(32) Jafri, J. A.; Logan, J.; Newton, M. D. *Isr. J. Chem.* **1980**, *19*, 340.

Table 3. Rms Deviations between the Crystal and Calculated Structures of Various Fe(III) Complexes[a]

	bond lengths[b]	bond angles[c]	torsion angles[c,d]
	In Vacuo		
Fe^{III}EHPG			
R,R	0.044	2.80	6.6
R,S	0.026	2.59	4.9
Fe^{III}TCTA	0.030	3.42	7.9
Fe^{III}TRDTA	0.024	2.90	12.3
trans-(O_5)-Fe^{III}EDDDA	0.027	3.82	17.2
	In Aqueous Solution[e]		
Fe^{III}EHPG			
R,R	0.044	3.15	6.9
R,S	0.025	2.78	5.5
Fe^{III}TCTA	0.032	2.98	6.3
Fe^{III}TRDTA	0.025	2.97	10.5
trans-(O_5)-Fe^{III}EDDDA	0.029	4.81	11.7

[a] Hydrogen atoms were excluded in these statistical analyses. [b] In units of ångstroms. [c] In units of degrees. [d] Torsion angles involved in linear bending angles around the metal center were not considered in these comparisons. [e] Solvent effects were calculated using the GB/SA model.

complexes have been the focus of several studies.[25,26,33,34] The EHPG ligand group contains four chiral atoms, specifically two carbon atoms and two nitrogen atoms. A total of 16 conformations could result from the chirality of these four atoms.

Another consideration is the conformation about the C–C bond in the $-CH_2-CH_2-$ groups linking the coordinating atoms. While either a *gauche* or *cis* conformation is conceivable, previous studies[34] confirm that the *cis* conformation will cause severe strain in the molecule. For this reason, it has not been observed under experimental conditions. The restriction of $-CH_2-CH_2-$ to a *gauche* conformation imposes a correlation between the two chiral nitrogen atoms: they will both assume either the *R* or *S* configuration. This constraint will also eliminate the possibility of mirror symmetry in the molecule, thus reducing the original 16 conformers to only 8.

In the four conformers with nitrogen atoms in the *R* configuration, the chiral carbon atoms can be labeled as (*R,R*), (*R,S*), (*S,R*), and (*S,S*). Since (*R,S*) and (*S,R*) are related by a 2-fold axis, only three of these four conformers differ in terms of interatomic distances and thus conformational energies. These conformers are shown in Figure 2. The corresponding four conformers with nitrogen atoms in the *S* configuration represent mirror images of the four *R* configurations. Accordingly, they are redundant configurations and were excluded from further investigation.

The 3 unique conformers among the original 16 provide a stringent test case for conformational studies insofar as the differences among them are purely configurational (i.e., geometrical) rather than chemical (i.e., atom types).

The Fe^{III}EHPG Complexes: Crystal Structures. The crystal structures for two distinct isomorphous forms of the (*R,R*)-*rac*-Fe^{III}EHPG complex have been reported.[25] These two forms vary somewhat in their crystal packing patterns since they were crystallized as different salts. A statistical analysis of their structural geometries reveals rms deviations of 0.032 Å in bond lengths, 1.76° in bond angles, and 5.4° in torsion angles. An *R,S meso* conformer was reported in the same work.

Energy-minimization calculations were carried out using our enhanced AMBER force field to optimize the structures both *in vacuo* and in aqueous solution. To quantify the effect of the polarizable solvent medium in an aqueous environment, we employed two separate procedures: (1) a crude estimate based on using a distance-dependent variable dielectric $\epsilon = \epsilon_0 R_{ij}$ (where

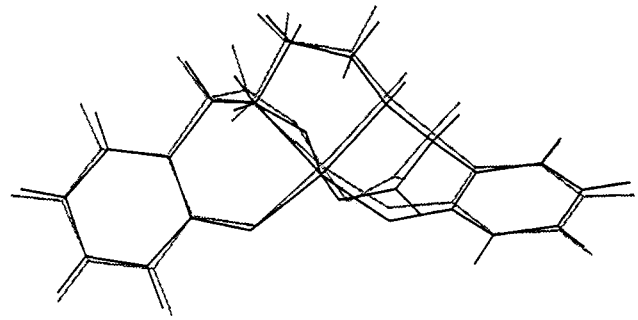

Figure 3. Superposition of the GB/SA calculated structure and the crystal structure (darker line) of the *R,R rac* conformer of the Fe^{III}EHPG complex.

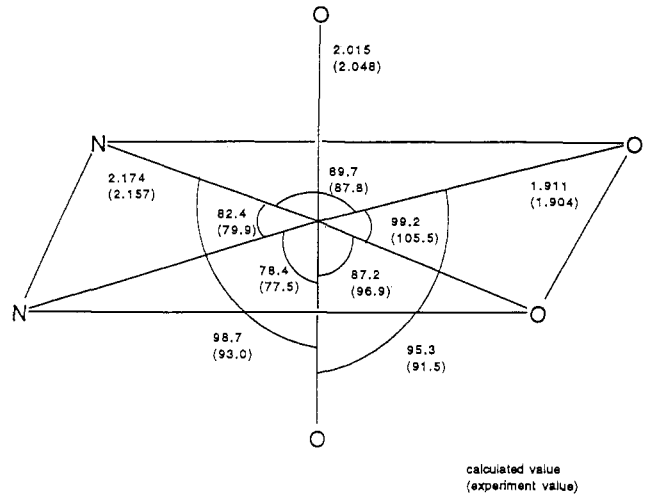

Figure 4. Calculated and X-ray crystallographic (in parentheses) values of the bond lengths and bond angles for the coordination sphere of the *R,R rac* conformer of the Fe^{III}EHPG complex.

$\epsilon_0 = 1.0$ and R_{ij} is the interatomic distance) which scales the Coulombic electrostatic term, and (2) the more robust continuum GB/SA solvation treatment of Still[35] based on computed surface areas (SA) and the generalized Born (GB) equation.

Deviations between the calculated and crystal-structure geometries arose chiefly from differences in the hydrogen positions. Considering that the MM calculations implicitly neglect the effects of crystal packing forces on geometry, the optimized structures reproduced their corresponding crystal structures reasonably well. A comparison of the calculated structures optimized *in vacuo* and in aqueous solution (GB/SA model) is summarized in Table 3. A superposition of the GB/SA-model calculated structure and corresponding crystal structure of the *R,R rac* conformer is given in Figure 3.

The crystal structures of the Fe^{III}EHPG complexes exhibit a somewhat distorted octahedral geometry. Specifically, the two O(phenolic)–Fe(III)–N bending angles deviate an average 17.0° from the perfect trans octahedral angle (180.0°). Accordingly, we assigned comparatively "soft" bending constants (15.0 kcal/(mol/rad^2)) to these bending angles around the metal center to achieve a better fitting to the flexible coordination geometry. A comparison of the calculated and crystal structure values of selected bond lengths and bond angles within the coordination sphere of the *R,R rac* conformer is shown in Figure 4.

The Fe^{III}EHPG Complexes: Energies. Tables 4a–c present a summary of the conformational energies of the Fe^{III}EHPG complexes calculated (a) *invacuo* ($\epsilon = 1.0$), (b) in aqueous solution using $\epsilon = \epsilon_0 R_{ij}$, and (c) in aqueous solution using the GB/SA

(33) Carrano, C. J.; Spartalian, K.; Appa Rao, G. V. N.; Pecoraro, V. L.; Sundaralingam, M. *J. Am. Chem. Soc.* **1985**, *107*, 1751.
(34) Riley, P. E.; Pecoraro, V. L.; Carrano, C. J.; Raymond, K. N. *Inorg. Chem.* **1983**, *22*, 3096.
(35) Still, W. C.; Tempczyk, A.; Hawley, R. C.; Hendrickson, T. *J. Am. Chem. Soc.* **1990**, *112*, 6127. Macromodel V3.0, Columbia University, Department of Chemistry, New York, 1990.

Table 4. Conformational Energies[a] of the Fe^{III}(EHPG) Complex

energy components	*R,R* conformer (*rac*)	*R,S* conformer (*meso*)	*S,S* conformer (*rac*)
a. In Vacuo[b]			
vdW nonbonded	3.55	3.00	1.59
stretching	1.90	2.78	3.20
bending	8.60	12.18	17.43
torsion	3.95	3.99	2.80
improper torsion	1.28	0.99	0.37
electrostatic[b]	−101.11	−94.21	−90.51
tot. energy	−81.83	−71.26	−65.11
relative energy	**0.00**	**10.57**	**16.72**
b. With Solvent Effects Treated Using a Distance-Dependent Dielectric[c]			
vdW nonbonded	2.74	2.44	1.74
stretching	1.44	2.27	3.04
bending	7.92	11.65	16.20
torsion	2.96	3.08	2.41
improper torsion	0.19	0.14	0.05
electrostatic[c]	−26.19	−24.63	−23.93
tot. energy	−10.93	−5.05	−0.49
relative energy	**0.00**	**5.88**	**10.44**
c. In Aqueous Solution with Solvent Effects Treated Using the GB/SA Model			
vdW nonbonded	2.40	2.27	1.91
stretching	2.32	3.28	4.44
bending	8.14	11.63	15.47
torsion	2.77	2.94	2.37
improper torsion	0.04	0.03	0.01
electrostatic[b]	−93.10	−87.19	−85.72
Solvation Terms			
$G_{cav+vdW}$	2.88	2.79	2.69
G_{pol}	−114.93	−122.34	−124.83
tot. energy	−189.48	−186.59	−183.66
relative energy	**0.00**	**2.89**	**5.82**

[a] In units of kcal/mol. [b] Electrostatic energies calculated using Coulomb's law with $\epsilon = 1.0$. [c] Electrostatic energies calculated using Coulomb's law with $\epsilon = \epsilon_0 R_{ij}$ and $\epsilon_0 = 1.0$.

model. The calculated results show that (1) the most stable conformation is the *R,R rac* conformer, while the least stable (i.e., highest conformational energy) conformation is the *S,S rac* conformer; (2) this order of energy preference does not change whether calculated *in vacuo* or in aqueous solution; and (3) aqueous solvation reduces the energy differences among the three conformers. Moreover, their differences in energy decrease significantly if the GB/SA model is used instead of the distance-dependent dielectric term $\epsilon = \epsilon_0 R_{ij}$ to simulate aqueous conditions.

While the *R,R rac* and *R,S meso* conformers are known to exist,[25] the *S,S rac* conformer has never been reported. Some workers[25] have ascribed the absence of the *S,S rac* conformer in the crystal to unfavorable crystal packing. Other workers[34] have claimed that the *S,S rac* conformer is inherently an unstable form. Consistent with the latter interpretation, our results for the aqueous GB/SA model indicate that the conformational energy of the *S,S rac* conformer is 5.82 kcal/mol higher than the *R,R rac* conformer (i.e., the most stable one) and 2.93 kcal/mol higher than the *R,S meso* conformer.

The calculated energy difference of 2.89 kcal/mol between the *R,R rac* conformer and the *R,S meso* conformer in aqueous solution (GB/SA model) is close to that deduced from experimental stability constants. In particular, the experimentally measured stability constants K_{ML} for the *rac* and *meso* complexes at 25 °C were reported, respectively, as $10^{35.0}$ and $10^{33.8}$ in one study[41] and as $10^{35.54}$ and $10^{33.28}$ in another study.[26] These values correspond to $\Delta(\Delta G)$ of 1.65 and 3.10 kcal/mol, respectively.

The Fe^{III}TCTA, Fe^{III}TRDTA, and Fe^{III}EDDDA Complexes. In order to derive a set of transferable force-field parameters, we also included Fe^{III}TCTA and Fe^{III}TRDTA among our basis set of fitting complexes. The Fe^{III}EDDDA [(ethylenediamine-*N,N'*-diaceto-*N,N'*-di-3-propionato)iron(III) ion] complex was added later to validate this parameter set. The structural geometry of each of these three complexes is illustrated in Figure 5.

The Fe^{III}TCTA complex contains a relatively rigid 1,4,7-triazanonane ring which makes it rather difficult for the ferric complex to adopt a regular octahedral geometry.[36] This is reflected primarily in the twist angle, ω, between the trigonal plane containing the three nitrogens and the plane containing the three oxygens. This angle would be 0.00° for a trigonal prismatic structure and 30.0° for a perfect octahedral structure. The twist angle in the crystal structure of Fe^{III}TCTA is only 12.6°.[36] The calculated structure retains the 3-fold axis observed in the crystal structure. The calculated values of ω, i.e., 16.7° in aqueous solution (GB/SA) and 17.7° *in vacuo*, agree reasonably well with the experimental value. This deviation from octahedral geometry is also reflected in the value of only 150° for the trans N–Fe–O bond angles in the crystal structure. The corresponding calculated value is 157.5° from both the GB/SA aqueous model and the *in vacuo* model, again in reasonably good agreement with the experimental value. The Fe^{III}TRDTA complex has a much more flexible structure with no symmetry. The overall rms deviations between the calculated and crystal structures of both Fe^{III}TCTA and Fe^{III}TRDTA are given in Table 3. The rms deviations in bond angles and bond lengths are about the same for the two complexes.

To test the generality of our force field parameter set, we investigated the Fe^{III}EDDDA complex in a similar manner. Analogous to the Fe^{III}EHPG complex, the Fe^{III}EDDDA complex has three types of coordinating atoms, viz., N atoms and two types of carboxylate O atoms. The possible conformers are depicted in Figure 6 as *trans*-(O_5), *trans*-(O_5,O_6), and *trans*-(O_6).[37] Of these three conformers, the *trans*-(O_5) conformer is the only one observed in the crystal.[38] We again calculated the energy differences among these conformers in aqueous solution. The results indicate that the *trans*-(O_5) and *trans*-(O_6) conformers are energetically the most and least stable conformers, respectively. The conformational energies of these conformers are listed in Table 5.

Discussion

It is well established that, with simple bidentate ligands, 5-membered chelate rings are more stable than the analogous 6-membered rings, e.g., complexes of ethylenediamine vs 1,3-diaminopropane. However, the bite distance is not ideal for either the 5-membered or 6-membered chelate ring. Internal ring strain thus diminishes the net stability of the metal chelate in both cases.[14] The observed difference in stability between 5- and 6-membered chelate rings is due in large part to lower strain in the 5-membered ring.[39]

A similar comparison of the relative stabilities of 5- and 6-membered chelate rings is not so simple in multidentate ligands. One observes that there are optimal combinations of 5- and 6-membered chelate rings. Table 6 shows a representative set of binding constants for copper(II) complexes for a series of tetraamines to illustrate this principle. In the (2,2,2) ligand, the short bite distance of the three 5-membered rings results in a cumulative strain energy. The insertion of a central 6-membered ring, with its longer bite distance, relieves this cumulative strain and leads to a substantial increase in the stability of the complex.

(36) Wieghardt, K.; Bossek, U.; Chaudhuri, P.; Herrmann, W.; Menke, B. C.; Weiss, J. *Inorg. Chem.* **1982**, *21*, 4308.
(37) (a) Radanovic, D. J.; Douglas, B. E. *Inorg. Chem.* **1974**, *14*, 6. (b) Helm, F. T.; Watson, W. H.; Radanovic, D. J.; Douglas, B. E. *Inorg. Chem.* **1977**, *16*, 2351.
(38) Yamamoto, T.; Mikata, K.; Miyoshi, K.; Yoneda, H. *Inorg. Chim. Acta* **1988**, *150*, 237.
(39) McDougall, G. J.; Hancock, R. D.; Boeyens, J. C. A. *J. Chem. Soc., Dalton* **1978**, 1438.
(40) Cramer, C. J.; Truhlar, D. G. *J. Am. Chem. Soc.* **1991**, *113*, 8305.

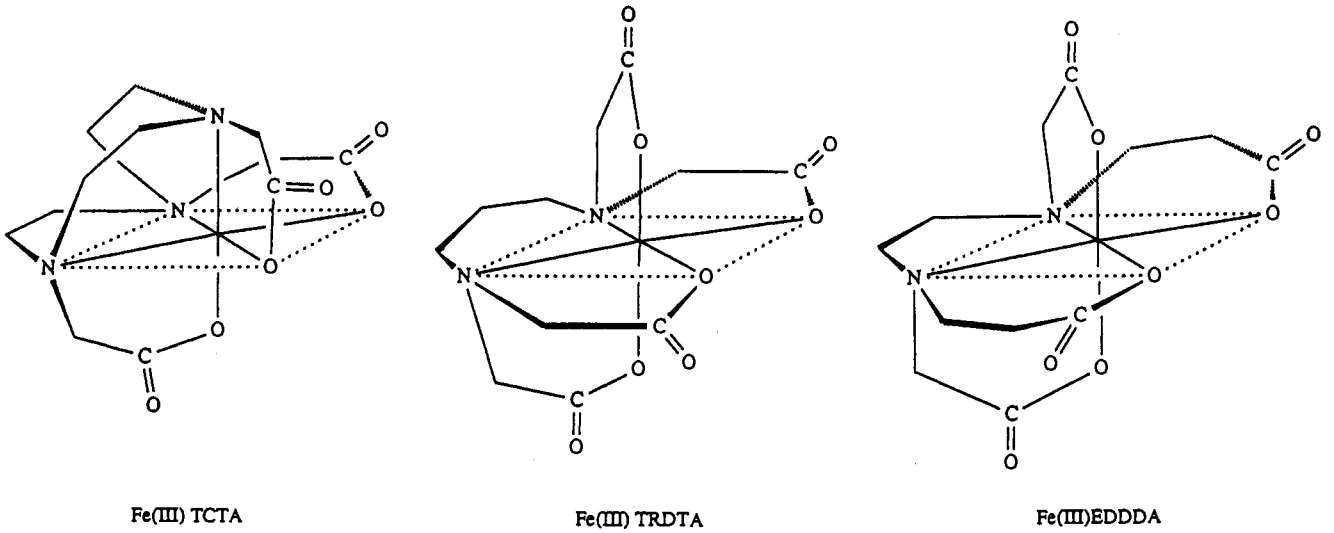

Figure 5. Illustration of the ferric complexes of triazacyclononane-1,4,7-triacetic acid (TCTA), 1,5-diazapentane-1,1,5,5-tetraacetic acid (TRDTA), and ethylenediamine-*N*,*N*′-diaceto-*N*,*N*′-di-3-propionic acid (EDDDA).

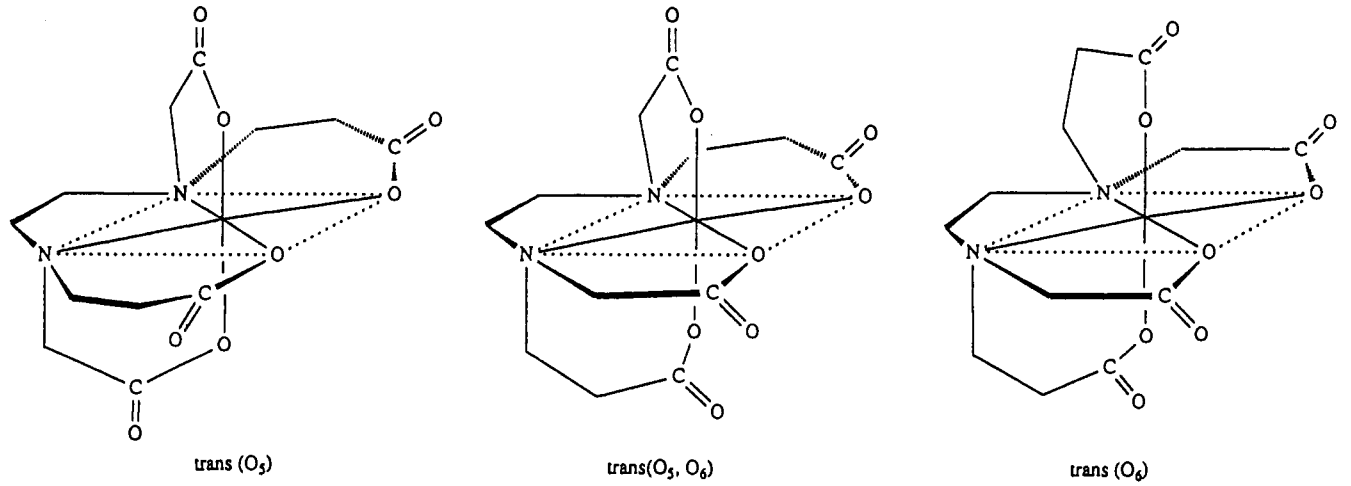

Figure 6. Illustration of the three Fe^{III}EDDDA conformers.

Table 5. Conformational Energies[a] of the Fe(III)EDDDA Complex in Aqueous Solution with Solvent Effects Treated Using the GB/SA Model

energy components	*trans*-(O_5)	*trans*-(O_5,O_6)	*trans*-(O_6)
vdW nonbonded	0.16	0.46	1.29
stretching	1.53	2.30	3.78
bending	8.04	13.08	20.34
torsion	10.25	9.94	9.33
improper torsion	0.30	0.20	0.11
electrostatic[b]	−53.36	−62.59	−69.06
	Solvation Terms		
$G_{cav+vdW}$	2.78	2.66	2.59
G_{pol}	−105.45	−98.34	−92.99
tot. energy	−135.74	−132.30	−124.62
relative energy	**0.00**	**3.44**	**11.12**

[a] In units of kcal/mol. [b] Calculated using Coulomb's law with $\epsilon = 1.0$.

The situation becomes progressively less favorable as more 6-membered rings are incorporated into the complex.

For the ferric complexes of both EHPG and EDDDA, the number of 5- and 6-membered chelate rings is fixed. Only their arrangement can change. The relative energies of the possible configurations for these complexes are given in Table 4 for EHPG and in Table 5 for EDDDA. The present MM calculations predict that the optimal stability will be achieved when the ligands adopt an equitorial coordination plane containing a 6,5,6 combination of chelate ring sizes, with two 5-membered axial chelate rings. This paradigm corresponds to the *R*,*R rac* conformer in the case of EHPG and to the *trans*-(O_5) conformer in the case of EDDDA.

Table 6. Copper(II) Binding Constants for a Series of Tetraamines: NH_2–$(CH_2)_x$–NH–$(CH_2)_y$–NH–$(CH_2)_z$–NH_2

x,*y*,*z*	$\log \beta_{110}$	$\Delta(\log \beta)$	$\Delta(\Delta G)$[a]
2,2,2	20.1	0	0
2,3,2	23.9	3.8	−5.2
3,2,3	21.7	1.6	−2.2
3,3,3	17.1	−2.4	+3.3

[a] In units of kcal/mol.

The present MM calculations fully support the concept that internal ring strain is a major factor in these energy differences. The more favorable energy of the *R*,*R rac* conformer *in vacuo* arises primarily from bond bending and, to a lesser extent, bond stretching and electrostatic terms. Relatively large solvation terms reduce the energy difference of 10.6 kcal/mol *in vacuo* to only 2.9 kcal/mol in aqueous solution (GB/SA model). The latter value is in good agreement with the experimental $\Delta(\Delta G)$ values of 1.65 and 3.1 kcal/mol.[26,41]

The importance of ring strain is further evidenced by comparing the stability constants of EHPG with the new ligand *N*,*N*′-trimethylenebis[2-(2-hydroxy-3,5-dimethylphenyl)glycine] (TMPHPG).[42] The primary structural difference between EHPG and TMPHPG is that the central ethylenediamine segment of

(41) Bernauer, K. *Top. Curr. Chem.* **1976**, *65*, 1.
(42) Bannochie, C. J.; Martell, A. E. *Inorg. Chem.* **1991**, *30*, 1385.

Table 7. Stability Constants for the (*R*,*R*) and (*R*,*S*) Complexes of EHPG[a]

metal ion	log $\beta_{110}(R,R)$	log $\beta_{110}(R,S)$	$\Delta(\Delta G)$[b]
Fe^{3+}	35.54	33.28	−3.1
Ni^{2+}	21.33	19.42	−2.6
Zn^{2+}	18.66	16.88	−2.4
Cu^{2+}	25.27	23.68	−2.2
Ga^{3+}	33.89	32.40	−2.0
In^{3+}	26.68	25.26	−2.0

[a] All data taken from ref 26. [b] In units of kcal/mol.

EHPG has been replaced by a propylenediamine group. Thus the central chelate ring has been increased from five to six atoms. For the *R*,*R rac* isomer, this changes the equitorial plane from a 6,5,6 combination of chelate rings for EHPG to a less favorable 6,6,6 combination for TMPHPG. Correspondingly, one observes that the *R*,*R rac* conformer of the ferric chelate of TMPHPG is 1.8 kcal/mol *less* stable than that of EHPG.[42] Conversely, the equatorial plane for the *R*,*S* isomer goes from a 5,5,6 combination for EHPG to a 5,6,6 combination for TMPHPG. In this case, one observes that the ferric complex of TMPHPG is 2.1 kcal/mol *more* stable than that of EHPG. There is a reversal in the relative stability of the conformers of each ligand such that the *R*,*S meso* complex is more stable for TMPHPG, while the *R*,*R rac* isomer is more stable for EHPG.

Stability constants for the *R*,*R rac* and *R*,*S meso* complexes of EHPG with several other metal ions have been determined.[26] As shown in Table 7, the *R*,*R* conformer is more stable by 2–3 kcal/mol for all the metal ions studied thus far. It is somewhat surprising that the relative stability of the *R*,*R rac* and *R*,*S meso* complexes varies by only 1 kcal/mol among the divalent and trivalent complexes of EHPG. Previous MM calculations on tetraazamacrocycles have shown that 6-membered chelate rings enhance the selectivity for smaller metal ions, while one observes that 5-membered chelate rings enhance the selectivity for larger metal ions.[14] However, there is no obvious correlation between the $\Delta(\Delta G)$ values in Table 7 and the ionic radius of the metal. The expected correlation may be obscured by ligand field effects for Cu^{2+} and Ni^{2+} and by Jahn–Teller effects for Cu^{2+}.

With regard to the energies calculated in this study, one should exercise caution in interpreting the breakdown of energy components appearing in Tables 4 and 5. One temptation is to attribute too much significance to the relative magnitude of the various component energies (e.g., bond-stretch vs bond-bending terms) for a single compound. Another temptation is to infer too much meaning from differences in a single energy component (e.g., electrostatics) across a series of compounds. It must be remembered that contemporary force fields are parameterized using least-square-fit procedures. Furthermore, the primary aim of these force-field parameterization schemes is to reproduce experimental or theoretical data. The chief aim is not to resolve the conformational energy into its discrete components. For this reason, the decomposition of the conformational energies into components should not be taken too literally. To illustrate this point, the *in vacuo* MM results in Table 4a indicate that the *R*,*R* and *S*,*S* conformers of Fe^{III}EHPG differ in conformational energy by 16.72 kcal/mol. In terms of energy components, the bond-angle bending term is shown to account for about 8.8 kcal/mol (or 53%) of this difference. One may safely conclude that bending energies play a significant role in dictating the differences in conformational energy between these two compounds. Just the same, it is unwarranted to claim that bending energies contribute 53% (or any other value) to the total conformational energy based on a strict decomposition of individual component energies. The high degree of interplay among the force field's individual terms and parameters invalidates any such literal accounting of the conformational energy.[45]

Experimental Section

These calculations were carried out using Macromodel V3.1[35] on the University's Digital VAX-VMS 8600 and 4200 computers. The *in vacuo* calculations computed the electrostatic energies from Coulomb's law with a fixed dielectric ϵ set to 1.0. To render a crude estimate of solvent effects, a second calculation was carried out using a distance-dependent dielectric expression $\epsilon = \epsilon_0 R_{ij}$ with $\epsilon_0 = 1.0$. We also applied the more rigorous continuum GB/SA solvation model (solvation model 3 in Macromodel[35]) developed by Still. This model adopts the generalized Born equation and treats the solvent as a continuum dielectric. It computes solvation free energies as the sum of two components: (1) a cavity plus van der Waals term $G_{cav+vdW}$, which is computed as a function of solvent-accessible surface area, and (2) an electrostatic polarization term G_{pol} calculated using a generalized Born (GB) model. The solvation free energy G_{sol} is then taken (see Table 5) as the sum $G_{sol} = G_{cav+vdW} + G_{pol}$. Since solvent polarization effects are treated explicitly by the GB/SA model, no special adjustment of the dielectric constant ϵ is required. Accordingly, an *in vacuo* dielectric of 1.0 was used for the Coulomb's law electrostatics term.

The reliability of the GB/SA model has been reported in other studies.[35,40] Various other force fields (i.e., MM3,[43] Discover[44]) were considered for the present study. However, our preliminary results indicated no clear superiority of one force field over the others in the present application. We chose the AMBER force field based on its popularity in applications to biological molecules such as transferrin, for which the Fe(III) complexes considered here serve as model systems. It should be noted that counterions were omitted in the present calculations of these Fe(III) complexes. The influence of counterions in determining the conformational behavior of either these model complexes or the corresponding transferrin complexes is likely secondary to the factors considered explicitly in the present analysis.

Acknowledgment. The authors gratefully acknowledge financial support from the National Institutes of Health (W.R.H., Grant DK35533; W.J.W., Grant CA47319). The authors also acknowledge Biosym Technologies, Inc., and Tripos Associates, Inc., for generous support in using their software.

(43) (a) Allinger, N. L.; Yuh, Y. H.; Lii, J.-H. *J. Am. Chem. Soc.* **1989**, *111*, 8551; (b) Lii, J. H.; Allinger, N. L. *J. Am. Chem. Soc.* 8566, 8576

(44) Insight/Discover, a product of Biosym Technologies, Inc., San Diego, CA.

(45) Welsh, W. J. In *Computational Modeling of Polymers*; Bicerano, J., Ed.; Marcel Dekker, Inc.: New York, 1992; pp 127–159.